The Astrophysical Journal Letters, 721:L53–L57, 2010 September 20 doi:10.1088/2041-8205/721/1/L53

THE ORIGIN OF ASTEROID 101955 (1999 RQ_{36})

Humberto Campins[1], Alessandro Morbidelli[2], Kleomenis Tsiganis[3], Julia de León[4], Javier Licandro[5,6], and Dante Lauretta[7]

[1] University of Central Florida, Physics Department, P.O. Box 162385, Orlando, FL 32816.2385, USA
[2] Departement Casiopée, Université de Nice–Sophia Antipolis, Observatoire de la Côte d'Azur, CNRS 4, 06304 Nice, France
[3] Department of Physics, Aristotle University of Thessaloniki, 54 124 Thessaloniki, Greece
[4] Instituto de Astrofísica de Andalucía-CSIC, Camino Bajo de Huétor 50, 18008 Granada, Spain
[5] Instituto de Astrofísica de Canarias (IAC), C/Vía Láctea s/n, 38205 La Laguna, Spain
[6] Department of Astrophysics, University of La Laguna, 38205 La Laguna, Tenerife, Spain
[7] Lunar and Planetary Laboratory, University of Arizona, Tucson, AZ 85721, USA
Received 2010 July 27; accepted 2010 August 10; published 2010 August 31

ABSTRACT

Near-Earth asteroid (NEA) 101955 (1999 RQ_{36}; henceforth RQ36) is especially accessible to spacecraft and is the primary target of NASA's OSIRIS-REx sample return mission; it is also a potentially hazardous asteroid. We combine dynamical and spectral information to identify the most likely main-belt origin of RQ36 and we conclude that it is the Polana family, located at a semimajor axis of about 2.42 AU. We also conclude that the Polana family may be the most important inner-belt source of low-albedo NEAs. These conclusions are based on the following results. (1) Dynamical evidence strongly favors an inner-belt, low-inclination (2.15 AU $< a <$ 2.5 AU and $i < 10^{\circ}$) origin, suggesting the ν_6 resonance as the preferred (95% probability) delivery route. (2) This region is dominated by the Nysa and Polana families. (3) The Polana family is characterized by low albedos and B-class spectra or colors, the same albedo and spectral class as RQ36. (4) The Sloan Digital Sky Survey colors show that the Polana family is the branch of the Nysa–Polana complex that extends toward the ν_6 resonance; furthermore, the Polana family has delivered objects of the size of RQ36 and larger into the ν_6 resonance. (5) A quantitative comparison of visible and near-infrared spectra does not yield a unique match for RQ36; however, it is consistent with a compositional link between RQ36 and the Polana family.

Key words: minor planets, asteroids: general

1. INTRODUCTION

The near-Earth asteroid (NEA) 101955 (1999 RQ_{36}; henceforth RQ36) is a particularly interesting object for several reasons. Its orbit makes it especially accessible to spacecraft and it is the primary target of NASA's OSIRIS-REx sample return mission (Lauretta et al. 2010). This object has also been identified as a potentially hazardous asteroid (Milani et al. 2009). The size shape and rotation state of this asteroid are well constrained. Radar observations indicate a diameter of approximately 580 m, a nearly spherical (spin-top) shape, and retrograde rotation with a period of 4.288 hr and the pole oriented nearly perpendicular to the orbit (Nolan et al. 2007). The spin-top shape and short rotation period are consistent with a Yarkovsky–O'Keefe–Radzievskii–Paddack (YORP) spin-up (Walsh et al. 2008). If so, the fine regolith on this asteroid may be concentrated near the equator or may have even been ejected. Although the current rotation period is too long for ejection of material from the surface, RQ36 might have spun down after the loss of material in the past. The nearly spherical shape can also be explained by recent close approaches with Earth (e.g., Richardson et al. 1998). Mid-infrared observations with NASA's *Spitzer Space Telescope* yield a thermal inertia consistent with a somewhat blocky surface and perhaps like that of the similarly sized NEA 25143 Itokawa (Emery et al. 2010).

Based on its visible spectrum this asteroid is classified as "B" (Clark et al. 2010b). B-class asteroids are found mostly in the middle and outer main belt and are believed to be primitive and volatile-rich. In fact, a comparison of the visible and near-infrared spectra of RQ36 with those of meteorites points to the most primitive meteorites (CIs and CMs) as the most likely analogs (Clark et al. 2010b). Furthermore, two large main-belt B-class asteroids have been linked to small asteroids that exhibit cometary behavior: (2) Pallas has been associated with NEA (3200) Phaethon (de León et al. 2010), and (24) Themis is related to the two "main-belt comets" in its dynamical family (Hsieh & Jewitt 2006). Moreover, water ice and organic molecules have been recently identified on the surface of (24) Themis (Campins et al. 2010; Rivkin & Emery 2010).

In this paper, we combine dynamical and spectral information to identify the most likely main-belt origin of RQ36. We use a similar approach to that of de León et al. (2010) and we conclude that the most likely source is the (142) Polana family, located at a semimajor axis ∼2.42 AU.

2. DYNAMICAL CONSTRAINTS

In this section, we first discuss dynamical considerations, which quickly restrict the likely source region of RQ36. Additional evidence, such as albedo, colors, possible family membership, and rotation state, strengthen the constraints from the dynamical arguments.

2.1. Likely Origins of the Current Orbit

The orbital elements of RQ36 are given in Table 1. Based on this orbit, it is possible to constrain the region of the main belt where it originated. A method for estimating the origin of near-Earth objects (NEOs) is described in Bottke et al. (2002). More specifically, they numerically integrated the orbits of thousands of test particles, starting from the five most efficient source regions of NEOs. These source regions are (1) the ν_6 secular resonance at ∼2.15 AU, which marks the inner border of the main belt, (2) the Mars-crossing asteroid population, adjacent to the main belt, (3) the 3:1 mean-motion resonance with Jupiter

Table 1
Osculating Orbital Elements at Epoch 2455400.5 (2010-Jul-23.0)[a]

Orbital Element	Value
Aphelion distance	1.356 AU
Perihelion distance	0.897 AU
Semimajor axis	1.126 AU
Eccentricity	0.204
Orbital period	1.20 yr
Mean anomaly	193.°42
Inclination	6.°04
Longitude of ascending node	2.°07
Argument of perihelion	66.°21

Note. [a] From NASA's Jet Propulsion Laboratory (http://ssd.jpl.nasa.gov/).

at 2.5 AU, (4) the outer main-belt population between 2.8 and 3.5 AU, and (5) the Jupiter-family comets. According to the Bottke et al. (2002) model for NEO sources, the orbit of RQ36 has a ∼95% probability to have been reached by objects that escaped through the ν_6 resonance, a ∼5% probability through the 3:1 mean-motion resonance with Jupiter, and a negligible chance to have originated further away from the Sun, including Jupiter-family comets. Furthermore, all ν_6 source orbits have initial inclinations lower than 10° and 50% of them lower than 5°. Note that an object arriving to the NEO space through the ν_6 resonance will roughly preserve its orbital inclination, since this secular resonance does not affect the inclination; this is not true for the 3:1 mean-motion resonance. These dynamical arguments strongly constrain the most likely source region to that of low-inclination orbits between the ν_6 and 3:1 resonances, which implies semimajor axes between 2.15 and 2.5 AU. These results essentially rule out two prominent families with similar visible spectra to that of RQ36 (Section 3), namely, the Pallas family (because of its high inclination[8] of ∼35° and larger semimajor axis) and the Themis family (because of its large semimajor axis of ∼3.1 AU).

2.2. Additional Considerations

A number of additional considerations strongly favor the Polana family as the likely source of RQ36.

2.2.1. Family Membership

A small asteroid like RQ36 is unlikely to be a primordial object because its collisional lifetime is much shorter than the age of solar system (Bottke et al. 2005). Thus, RQ36 must be the fragment of a larger object. In looking for its parent body, asteroid families are much favored over single objects as the likely source. This is because in asteroid families numerous small fragments of the size of RQ36 have been produced during the family-forming event. Conversely, single objects, which do not have an observable family around them, either never broke up or generated too few and too small fragments to be observed. Therefore, we focus our search in this work on asteroid families only.

[8] Specifically for the Pallas family, since it is the most likely source of NEA 3200 Phaethon (de León et al. 2010) we looked into the possibility that high-inclination NEAs coming from the Pallas region can evolve into "RQ36-like" low-inclination orbits, under the perturbations of the terrestrial planets. Performing a numerical integration of 30 clones of 3200 Phaethon for 1 My, we found that the probability to reach an orbit with $i < 10°$ is negligible.

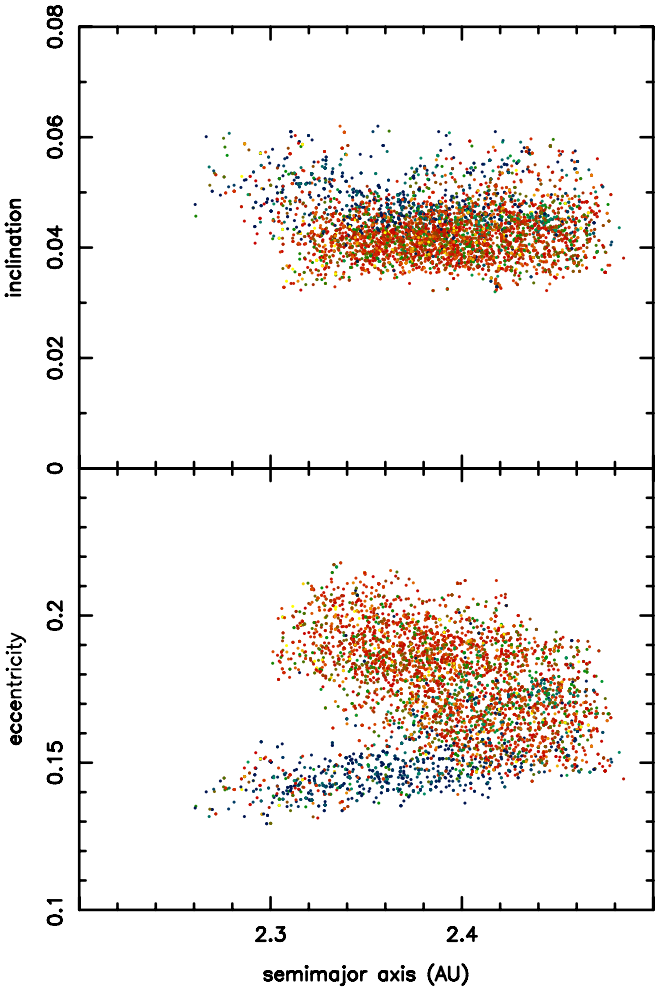

Figure 1. Distribution of the Nysa–Polana complex in the space of proper semimajor axis, eccentricity, and inclination. The colors in this figure represent the Sloan Digital Sky Survey (SDSS) colors (Parker et al. 2008). While the Nysa and Polana families overlap considerably in the (a, i) plot, they overlap only beyond 2.4 AU in the (a, e) plot. The Polana family (the structure at lower eccentricity in the bottom panel) is dominated by "blue" primitive-like objects, while the Nysa family is dominated by "red-yellow" S-class objects.

After excluding families like those of (4) Vesta and (8) Flora, whose composition is clearly inconsistent with RQ36, the source region defined by the dynamical constraints is dominated by two asteroid families, centered at a ∼2.42 AU, which partially overlap in the proper orbital parameter space, namely, Nysa and Polana (e.g., Cellino et al. 2002). Because of the difficulties in disentangling them on the basis of the orbital element distribution, these two families are often referred to as the Nysa–Polana complex. However, these families are clearly distinct from each other if the reflectance colors of their members are also considered, as shown in Figure 1.

2.2.2. Albedo

The sample of asteroids with measured albedos is considerably smaller than the number for which SDSS colors are available. Nevertheless, the average value for the geometric albedo of Polana family asteroids observed so far is 5.5% ± 1.5% (Davis & Neese 2002), which is consistent with the range of values, 3%–6%, estimated for RQ36 (Emery et al. 2010).

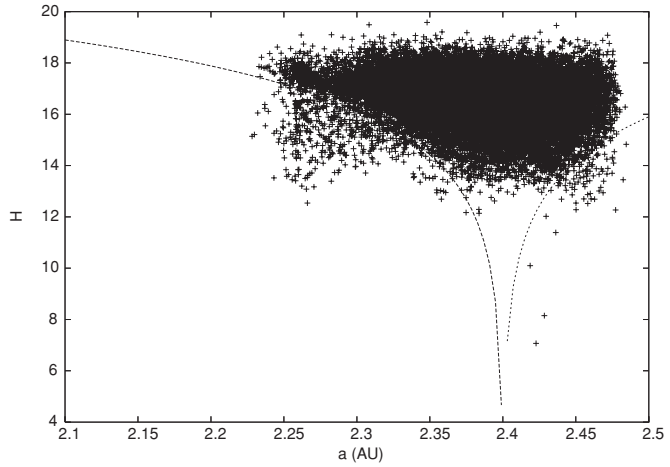

Figure 2. H_v vs. a_p plot for the Nysa–Polana complex. The dashed lines show the H_v-dependent semimajor axis distribution induced by the Yarkovsky effect that best fits the boundaries of the observed distribution. Bodies below these curves are expected to be interlopers, i.e., not genetically linked to either Nysa or Polana. The extrapolated Yarkovsky-induced distribution predicts that the Nysa–Polana complex should reach the outer edge of the ν_6 resonance for objects with $H_v \sim 18.5$, which for a Polana-like albedo of $p_v = 5\%$ translates into a diameter $D \sim 2$ km.

2.2.3. Spectral Type

At visible wavelengths, the Polana family is characterized by B-class spectra or colors, which is the same spectral class as RQ36. In contrast, the Nysa family consists of objects with visible colors (and albedos) totally inconsistent with those of RQ36; we elaborate on this point in Section 3. Furthermore, there are no other potential families (with low albedo and B-class spectra), contained within the ν_6 and the 3:1 resonances.

2.2.4. Transport to Resonance

Polana-family asteroids of sizes equal to and larger than RQ36 have reached the ν_6 resonance. This can be shown as follows. The absolute magnitude (H_v) versus semimajor axis plot of the Nysa–Polana complex (Figure 2) appears to be "V"-shaped, a feature known to be associated both with the size-dependent ejection velocity field and with the drift in the proper semimajor axis "a_p" induced by the Yarkovsky effect (e.g., Vokrouhlický et al. 2006). The dashed curves in the figure show the H-dependent semimajor axis distribution induced by the Yarkovsky effect that best fits the boundaries of the observed distribution. Bodies below these curves are expected to be interlopers, i.e., not genetically linked to either Nysa or Polana. Comparing these curves with the observed distribution, we remark that (1) on the right-hand side, the Nysa–Polana complex abruptly terminates at 2.48 AU, the location of the inner edge of the 3:1 mean-motion resonance with Jupiter (which is a possible, but not very likely source of the orbit of RQ36; Section 2.1) and (2) on the left-hand side no abrupt termination is observed;[9] instead, the extrapolated Yarkovsky-induced distribution predicts that the Nysa–Polana complex should reach the outer edge of the ν_6 resonance (at ~2.15 AU for the inclination of 2°.5 characteristic of this family; Morbidelli & Gladman 1998) for objects with $H_v \sim 18.5$. We stress that this estimate refers specifically to the Polana family rather than generically to the Nysa–Polana complex, because the observed distribution inside of 2.3 AU is entirely due to Polana family members (Figure 1). A magnitude $H_v = 18.5$, for a Polana-like albedo of $p_v = 5\%$, translates into a diameter $D \sim 2$ km, i.e., more than three times larger than RQ36. Thus, many RQ36-sized Polana family fragments should have already reached the ν_6 resonance. Those that did presumably had their orbital eccentricities increased to values that would render them Mars- or even Earth-crossers (Bottke et al. 2002), most preserving their original small inclinations.

[9] What causes the lack of Polana members between the ν_6 resonance and ~ 2.24 AU is likely an observational selection effect on objects too small to be properly observed.

2.2.5. Retrograde Rotation

In order for the Yarkovsky effect to move objects from the Polana region into the ν_6 resonance, their rotation has to be retrograde (so that $da/dt < 0$) and RQ36 is retrograde (Nolan et al. 2007). However, the spin axis of this asteroid could have changed either due to small impacts while the object was in the main belt or due to the YORP effect. So, the current spin state of RQ36 does not necessarily constrain what it was when the family was formed. Nevertheless, its current spin axis orientation is consistent with what was needed for it to be transported inward into the ν_6 resonance.

We believe these arguments make a strong case in favor of the Polana family as the most likely source of RQ36 via the ν_6 resonance.

3. SPECTRAL COMPARISONS

To explore a compositional connection between RQ36 and its likely main-belt origin, we have compiled the relevant spectra. The visible spectrum (0.45−0.92 μm) of RQ36 is from Clark et al. (2010b). The visible spectrum of Polana is from the Small Main-Belt Asteroid Spectroscopic Survey (SMASS; Bus & Binzel 2002b). The near-infrared spectrum (0.8−2.5 μm) of RQ36 is from the MIT–Hawaii–IRTF Joint Campaign for NEO Spectral Reconnaissance (Binzel et al. 2005). The near-infrared spectrum of (142) Polana is from an ongoing observational program led by the authors of this work and focused on the acquisition of near-infrared spectra of main-belt B-class asteroids (J. de León et al. 2010, in preparation). Visible and near-infrared spectra of other relevant families, namely, the Pallas and Themis families, are also from these databases, our observational program, or the published literature (Clark et al. 2010a; de León et al. 2010; Binzel 2008).

As expected, the visible spectrum alone shows similarities between RQ36 and B-class families, including the Polana and Themis families, and less so with the Pallas family. However, as discussed in Section 2, dynamical considerations rule out the Pallas and Themis families.

On the other hand, the near-infrared spectrum of RQ36 (Figure 3) seems unique so far, and its implications are not clear. The near-infrared spectrum (0.8–2.0 μm) starts with a slope similar to that in the visible, has an inflection near 1.2 μm, and then a slight negative slope toward longer wavelengths. Interestingly, near-infrared spectra are quite diverse among B-class asteroids[10] (e.g., Clark et al. 2010a; de León et al. 2010). At these wavelengths, RQ36 is different from (2) Pallas, (24) Themis, (142) Polana and their families, and also different from NEA (3200) Phaethon. One could say that the near-infrared

[10] The compositional explanation for this spectral similarity at visible wavelengths and diversity in the near-infrared is not yet understood; it could be related to the abundance, or lack, of hydrated minerals. Hydrated silicates have been identified in (2) Pallas (Rivkin et al. 2002), but are absent on the surface of (24) Themis (Campins et al. 2010; Rivkin & Emery 2010).

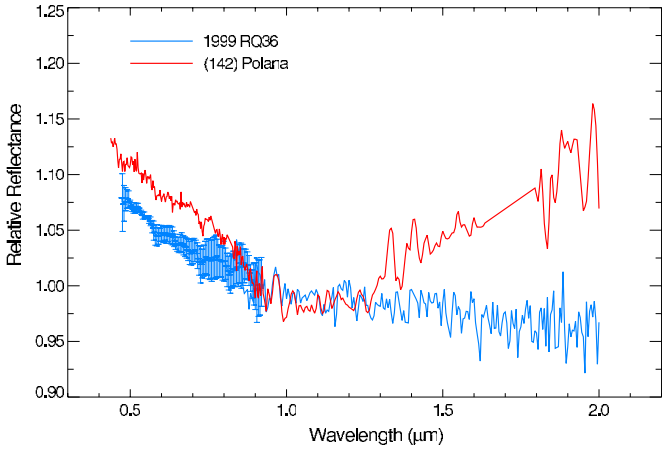

Figure 3. Relative reflectance spectra of asteroids 1999 RQ_{36} and (142) Polana at visible and near-infrared wavelengths, normalized to 1.0 reflectance at 0.9 μm. These spectra are truncated at 2 μm because RQ36 is close to the Sun and has a thermal contribution starting at approximately 2.1 μm. As stated in Section 3, although a quantitative spectral analysis does not yield a unique match, it is consistent with a compositional link between RQ36 and the Polana family.

spectrum of RQ36 has an intermediate shape between extremes represented by (24) Themis on one end and (2) Pallas on the opposite (Clark et al. 2010a).

We have carried out a quantitative comparison of all the available spectra in the visible and near-infrared. Following a similar approach as in de León et al. (2010), we used a χ^2 test to compare the complete spectra of RQ36 with the visible and near-infrared spectra of a total of 27 main-belt B-type asteroids. All spectra were normalized to unity at 0.9 μm, and the comparison extended up to 2.1 μm in the near-infrared. The smaller the value of χ^2 the more similar the spectra are. The best and the worst matches corresponded to $\chi^2 = 1.33$ and $\chi^2 = 105.06$, respectively. Asteroid (142) Polana has a $\chi^2 = 4.91$, which translates into a 92% similarity, and places it within the 10 objects whose spectra differ from the spectrum of RQ36 by only a 10%. Interestingly, 3 of those 10 best matches belong to the Themis family and another 3 to the Pallas family; however, both of these families are ruled out by dynamical considerations. Although this analysis does not yield a unique match (as was the case of 3200 Phaethon and the Pallas family; de León et al. 2010), it is consistent with a compositional link between RQ36 and the Polana family. Nevertheless, we emphasize that the sample of B asteroids with near-infrared spectra is rather limited, and more observations are necessary for a more conclusive result on the spectral links.

In some cases, the surface mineralogy of asteroids can be well constrained by spectral features, for example, the S-class asteroids in the Nysa family are compositionally inconsistent with the low albedo and relatively featureless spectrum of RQ36. However, the near-infrared spectral difference between RQ36 and (142) Polana does not necessarily imply a different origin. There are several possible reasons for a spectral difference between RQ36 and (142) Polana.

1. *Close approaches with Earth.* These approaches may have exposed fresh material and possibly even turned the body "inside out" (e.g., Binzel et al. 2010). Indeed our numerical integration of 30 clone orbits for RQ36 shows that, on average, this NEA has ~5 encounters with the Earth, within the Earth–Moon distance, per 100,000 years. Therefore, the surface of RQ36 is likely very fresh compared with that of (142) Polana. Although the effect of space weathering on the infrared spectra of primitive asteroids is not well characterized yet (e.g., Brunetto 2009), it is a plausible explanation for the observed spectral differences.
2. *Differences in the regolith grain size.* It appears that smaller asteroids are covered with coarser grains. This is consistent with results, showing that smaller asteroids have higher thermal inertia (Delbó et al. 2007). Large objects, such as (142) Polana (diameter = 55 km), tend to have lower thermal inertia because of their finer-grained surface. Smaller objects such as RQ36 likely lost any original regolith during the collisional event that created them, and are not able to develop or retain a new regolith, thus keeping preferentially larger grains on their surfaces. In addition, electrostatic dust levitation may contribute to the loss of the smaller grains in the lower gravity environment of smaller asteroids. However, the effect of particle size on the spectral structure at these wavelengths and on this type of spectrum has not been characterized. Therefore, the relevance of any regolith grain size difference between these two objects to their spectral differences is not yet clear.
3. *Spin state.* As mentioned in Section 1, the spherical shape, the orientation of the spin axis, and the short rotation period of RQ36 are consistent with a YORP spin-up (Walsh et al. 2008). If so, the fine regolith on this asteroid may be concentrated near the equator or may have even been ejected.

The conclusion of this section is that the albedo and the spectra favor the Polana family and rule out other inner main-belt ($a < 2.5$ AU) sources for RQ36. The dynamical arguments, which also strongly favor the Polana family, rule out the rest of the main-belt ($a > 2.5$ AU) and the Jupiter-family comets.

4. CONCLUSIONS

The Polana family is the most likely main-belt origin of RQ36.

1. The dynamical evidence discussed is Section 2 very strongly favors an inner main-belt, low-inclination (2.15 AU $< a <$ 2.5 AU and $i < 10^\circ$) origin for RQ36, the ν_6 resonance as the preferred (95% probability) delivery route.
2. This region is dominated by the Nysa and Polana families, and asteroid families are favored over a single object as likely sources because, in asteroid families, numerous small fragments (the size of RQ36) have already been produced.
3. The Polana family is characterized by B-class spectra or colors at visible wavelengths, which is the same spectral class as RQ36. In contrast, the Nysa family consists of objects with visible colors and spectra inconsistent with those of RQ36.
4. The SDSS colors of these two families show that the Polana family is the branch of the Nysa–Polana complex that extends toward the ν_6 resonance (Figure 1). Furthermore, a plot of absolute magnitude versus semimajor axis (Figure 2) shows that the Polana family has delivered objects of the size of RQ36 and larger into the ν_6 and 3:1 resonances.
5. In order for the Yarkovsky effect to move objects from Polana into the ν_6 resonance, they have to have retrograde rotation, and the spin of RQ36 is retrograde.
6. A quantitative comparison of visible and near-infrared spectra does not yield a unique match for RQ36; however, it is consistent with a compositional link between RQ36 and the Polana family.

Finally, our results suggest that the Polana Family is an important source of low-albedo, B-type material to near-Earth space, and likely the most important inner-belt source of low-albedo material.

H.C. acknowledges support from NASA's Planetary Astronomy program and from the National Science Foundation. H.C. was a visiting astronomer at the Observatoire de la Côte d'Azur, Nice, France, and at the "Instituto de Astrofísica de Canarias" in Tenerife, Spain. J.deL. and J.L. gratefully acknowledge support from the Spanish "Ministerio de Ciencia e Innovación" projects AYA2005-07808-C03-02 and AYA2008-06202-C03-02. Part of the data utilized in this publication were obtained and made available by the MITUH-IRTF Joint Campaign for NEO Reconnaissance. The IRTF is operated by the University of Hawaii under Cooperative Agreement No. NCC 5–538 with the National Aeronautics and Space Administration, Office of Space Science, Planetary Astronomy Program. The MIT component of this work is supported by the National Science Foundation under grant 0506716. We benefited from helpful comments from Marco Delbó, Zoe Landsman and Patrick Michel.

REFERENCES

Binzel, R. P., Rivkin, A. S., Thomas, C. A., DeMeo, F. E., Tokunaga, A., & Bus, S. J. 2005, in LPI Tech. Rep. 36, The MIT-Hawaii-IRTF Joint Campaign for NEO Spectral Reconnaissance, ed. S. Mackwell & E. Stansbery (Houston: LPI), 1817
Binzel, R. 2008, in LPI Contribution No. 1405, Spectral Properties of Near-Earth Object Mission Targets, ed. LPI Ed. Board (Houston: LPI), 8228
Binzel, R. P., et al. 2010, Nature, 463, 331
Bottke, W. F., Durda, D. D., Nesvorný, D., Jedicke, R., Morbidelli, A., Vokrouhlický, D., & Levison, H. 2005, Icarus, 175, 111
Bottke, W. F., Morbidelli, A., Jedicke, R., Petit, J.-M., Levison, H. F., Michel, P., & Metcalfe, T. S. 2002, Icarus, 156, 399
Brunetto, R. 2009, Earth Moon Planets, 105, 249
Bus, S. J., & Binzel, R. P. 2002a, Icarus, 158, 146
Bus, S. J., & Binzel, R. P. 2002b, Icarus, 158, 106
Campins, H., et al. 2010, Nature, 464, 1320
Cellino, A., Bus, S. J., Doressoundiram, A., & Lazzaro, D. 2002, in Asteroids III, ed. W. F., Jr., Bottke, A. Cellino, P. Paolicchi, & R. P. Binzel (Tucson, AZ: Univ. Arizona Press), 633
Clark, B. E., et al. 2010a, J. Geophys. Res., 115, E06005
Clark, B. E., et al. 2010b, Icarus, submitted
Davis, D. R., & Neese, C. (ed.) 2002, Asteroid Albedos, EAR-A-5, DDR-ALBEDOS-V1.1, NASA Planetary Data System, http://sbn.psi.edu/pds/resource/albedo.html
Delbó, M., Dell'Oro, A., Harris, A. W., Mottola, S., & Mueller, M. 2007, Icarus, 190, 236
de León, J., Campins, H., Tsiganis, K., Morbidelli, A., & Licandro, J. 2010, A&A, 513, A26
Emery, J. P., Fernández, Y. R., Kelley, M. S., Hergenrother, C., Ziffer, J., Lauretta, D. S., Drake, M. J., & Campins, H. 2010, in LPI Contribution No. 1533, ed. LPI Ed. Board (Houston: LPI), 2282
Hsieh, H. H., & Jewitt, D. 2006, Science, 312, 561
Lauretta, D. S., et al. 2010, in 73rd Annual Meteoritical Society Meeting, http://www.lpi.usra.edu/meetings/metsoc2010/pdf/5153.pdf
Milani, A., Chesley, S. R., Sansaturio, M. E., Bernardi, F., Valsecchi, G. B., & Arratia, O. 2009, Icarus, 203, 460
Morbidelli, A., & Gladman, B. 1998, Meteorit. Planet. Sci., 33, 999
Nolan, M. C., Magri, C., Ostro, S. J., Benner, L. A., Giorgini, J. D., Howell, E. S., & Hudson, R. S. 2007, BAAS, 39, 433
Parker, A., Ivezić, Ž., Jurić, M., Lupton, R., Sekora, M. D., & Kowalski, A. 2008, Icarus, 198, 138
Richardson, D. C., Bottke, W. F., & Love, S. 1998, Icarus, 134, 47
Rivkin, A. S., & Emery, J. P. 2010, Nature, 464, 1322
Rivkin, A. S., Howell, E. S., Vilas, F., & Lebofsky, L. A. 2002, in Asteroids III, ed. W. F., Jr., Bottke et al. (Tucson, AZ: Univ. Arizona Press), 635
Vokrouhlický, D., Brož, M., Bottke, W. F., Nesvorný, D., & Morbidelli, A. 2006, Icarus, 182, 118
Walsh, K. J., Richardson, D. C., & Michel, P. 2008, Nature, 454, 188